Chapter 2
Introduction to Extremum Seeking

In this chapter, we review the motivation behind extremum seeking methodology and the advances in the field of extremum seeking of the last 15 years. Then we present a basic introduction to stochastic extremum seeking, including how it relates to standard deterministic extremum seeking with periodic perturbations and what ideas are behind the study of stability of the resulting stochastic nonlinear system.

2.1 Motivation and Recent Revival

Extremum seeking is a non-model based real-time optimization approach for dynamic problems where only limited knowledge of a system is available, such as when the system has a nonlinear equilibrium map which has a local minimum or maximum. Popular in applications around the middle of the twentieth century, extremum seeking was nearly dormant for several decades until the emergence of a proof of its stability [71], with a subsequent resurgence of interest in extremum seeking for further theoretical developments and applications.

The increasing complexity of engineering systems, including feedback systems, has led to many optimization challenges since analytic solutions to optimization problems for multi-agent, nonlinear, and infinite-dimensional systems are difficult, if not impossible, to obtain. This difficulty arises for many reasons, including the presence of competing or adversarial goals, the high-dimensionality of the system, and the inherent system uncertainty. Moreover, if a model-based solution is obtained for these complicated optimization problems, it is likely to be conservative due to modeling deficiencies. Hence, non-model based extremum seeking methods are an attractive option to solve these problems.

Many works have focused on optimization/learning methods for unknown systems in a wide variety of fields. In games, most algorithms designed to achieve convergence to Nash equilibria require modeling information for the game and assume the players can observe the actions of the other players. The fictitious play strategy is one such strategy (employed in finite games) where a player devises a best

S.-J. Liu, M. Krstic, *Stochastic Averaging and Stochastic Extremum Seeking*, Communications and Control Engineering,
DOI 10.1007/978-1-4471-4087-0_2, © Springer-Verlag London 2012

response based on the history of the other players actions. A dynamic version of fictitious play and gradient response is developed in [126] and shown to converge to a mixed-strategy Nash equilibrium in cases where previously developed algorithms did not converge. In [38], regret testing with random strategy switches is proved to converge to the Nash equilibrium in finite two-player games where each player measures only its own payoffs. In [150], a synchronous distributed learning algorithm, where players remember their own actions and utility values from the previous two times steps, is shown to converge in probability to a set of restricted Nash equilibria. In [8, 48, 128], games with a continuum of traders are analyzed. Additional results on learning in games can be found in [26, 37, 42, 54, 83, 127].

The extremum seeking (ES) method has seen significant theoretical advances during the past decade, including the proof of local convergence [6, 27, 119, 140], PID tuning [61], slope seeking [7], performance improvement and limitations in ES control [70], extension to semi-global convergence [137], development of scalar Newton-like algorithms [101, 102, 108], inclusion of measurement noise [135], extremum seeking with partial modeling information [1, 2, 33, 36, 50], and learning in noncooperative games [40, 136].

ES has also been used in many diverse applications with unknown/uncertain systems, such as steering vehicles toward a source in GPS-denied environments [28, 30, 146], active flow control [15, 16, 24, 53, 63, 64], aeropropulsion [104, 144], colling systems [82, 84] wind energy [32], photovoltaics [81], human exercise machines [148], optimizing the control of nonisothermal valve actuator [113], controlling Tokamak plasmas [25], and enhancing mixing in magnetohydrodynamic channel flows [96], timing control of HCCI engine combustion [62], formation flight optimization [20], control of aircraft endurance based on atmospheric turbulence [69], beam matching adaptive control [123], optimizing bioreactors [141], control of combustion instability [9], control of nonisothermal continuous stirred reactors [49], control of swirl-stabilized spray combustion [105], optimal control of current profile in the DIII-D tokamak [110], laser pulse shaping [115], control of beam envelope in particle accelerators [122], control of an axial-flow compressor [142], and stabilization of neoclassical tearing modes in tokamak fusion plasmas [143].

2.2 Why Stochastic Extremum Seeking?

In existing perturbation-based extremum seeking algorithms, periodic (sinusoidal) excitation signals are primarily used to probe the nonlinearity and estimate its gradient. Biological systems (such as bacterial chemotaxis) do not use periodic probing in climbing food or light gradients. In man-made source seeking systems, the nearly random motion of the stochastic seeker has its advantage in applications where the seeker itself may be pursued by another pursuer. A seeker, which successfully performs the source finding task but with an unpredictable, nearly random trajectory, is a more challenging target, and is hence less vulnerable, than a deterministic seeker. Furthermore, if the system has high dimensionality, the orthogonality requirements

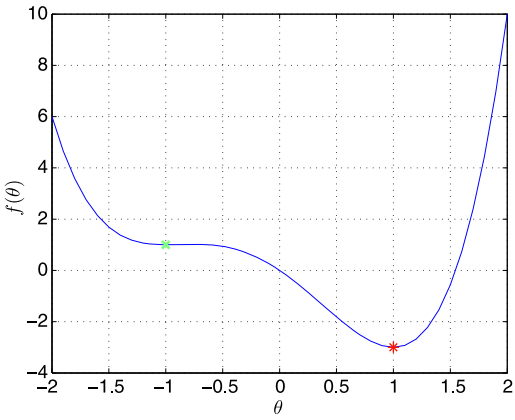

Fig. 2.1 A quartic static map with local minimum $f(-1) = 1$ and global minimum $f(1) = -3$

on the elements of the periodic perturbation vector pose an implementation challenge. Thus there is merit in investigating the use of stochastic perturbations within the ES architecture. The first results in that direction were achieved in the discrete-time case [98], using the existing theory of stochastic averaging in the discrete-time case. Source seeking results employing deterministic perturbations in the presence of stochastic noise have been reported in [133, 134], also in discrete time.

Stochastic extremum seeking and its stability analysis have some ideas and techniques in common with classical methods of annealing, stochastic approximation, and stochastic adaptive control [14, 43, 44, 75, 93–95].

2.3 A Brief Introduction to Stochastic Extremum Seeking

In this section, we present the basic idea of stochastic extremum seeking, make a comparison with deterministic (periodically perturbed) extremum seeking, and discuss a heuristic idea of stochastic averaging as a way of studying stability of a stochastic extremum seeking algorithm.

While extremum seeking is applicable to plants with dynamics (plants modeled by ordinary differential equations), in this section we introduce extremum seeking on the simplest possible problem—the optimization of a static map $f(\theta)$. Without loss of generality, we assume that f has a minimum at $\theta = \theta^*$ and we seek that minimum.

For the purpose of illustration, we use the following quartic map

$$f(\theta) = \theta^4 + \theta^3 - 2\theta^2 - 3\theta, \tag{2.1}$$

which is depicted in Fig. 2.1 and has a local minimum $f(-1) = 1$ and a global minimum $f(1) = -3$. The second derivatives at the two minima are $f''(-1) = 2 < 14 = f''(1)$, which is consistent with the global minimum at $\theta = 1$ being much "deeper" and "sharper" than the local minimum at $\theta = -1$.

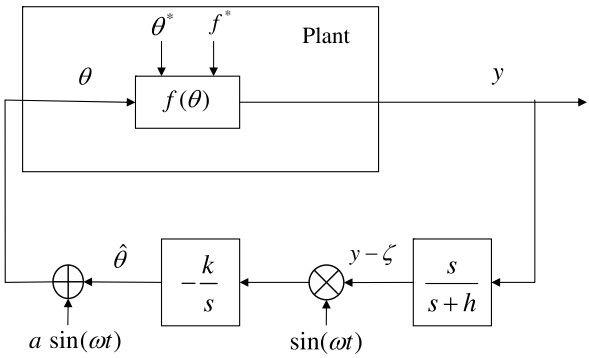

Fig. 2.2 Block diagram for *deterministic* extremum seeking scheme for a static map

2.3.1 A Basic Deterministic ES Scheme

Let us consider first the deterministic ES scheme shown in Fig. 2.2. The scheme employs a sinusoidal perturbation $\sin(\omega t)$, which additively enters the map $f(\theta)$. The measured output $y = f(\theta)$ is then passed through a washout filter and multiplied by the same perturbation signal, $\sin(\omega t)$, generating an estimate of the derivative (scalar gradient) $f'(\theta)$ at the input of the integrator. The integrator then updates the estimate $\hat{\theta}(t)$ in the direction of driving the gradient to zero. For $k > 0$ the ES scheme drives $\hat{\theta}(t)$ toward the nearest local minimum of $f(\theta)$, whereas for $k < 0$ the scheme converges toward the nearest maximum. The washout filter $\frac{s}{s+h}$ is not required but it helps performance somewhat. The logic behind the use of the washout filter is to kill the DC component of the map, $f(\theta^*)$, although the multiplication of the output y with the zero-mean perturbation $\sin(\omega t)$ also performs that role. The washout filter is just more effective in eliminating the DC component of y, without requiring that the perturbation frequency ω be relatively high.

The scheme in Fig. 2.2 has four design parameters, a, k, ω, and h. The amplitude a provides a trade-off between asymptotic performance and the region of attraction of the algorithm. The smaller the a, the smaller the residual error at the minimum achieved, but also the larger the possibility of getting stuck at a local minimum. Conversely, the larger the a, the larger both the residual error and the possibility of reaching the global minimum. The gain parameter k controls the speed of convergence, jointly with a which also influences the speed of convergence. The perturbation frequency ω controls the separation between the time scale of the estimation process, conducted by the integrator, and of the gradient estimation process, performed by the additive and multiplicative perturbation. The higher the frequency ω, the cleaner the estimate of the gradient and the smaller the effect of the perturbations introduced by the higher-order harmonics and of the DC component of y. The washout filter frequency h should be smaller than ω, so that the filter eliminates the DC component in y without corrupting the estimation of the gradient $f'(\theta)$.

Figure 2.3 shows the time response of a discrete-time version of the deterministic ES algorithm in Fig. 2.2. Even though the algorithm starts from the local minimum $\theta = -1$, it does not remain stuck at the local minimum and converges to the global

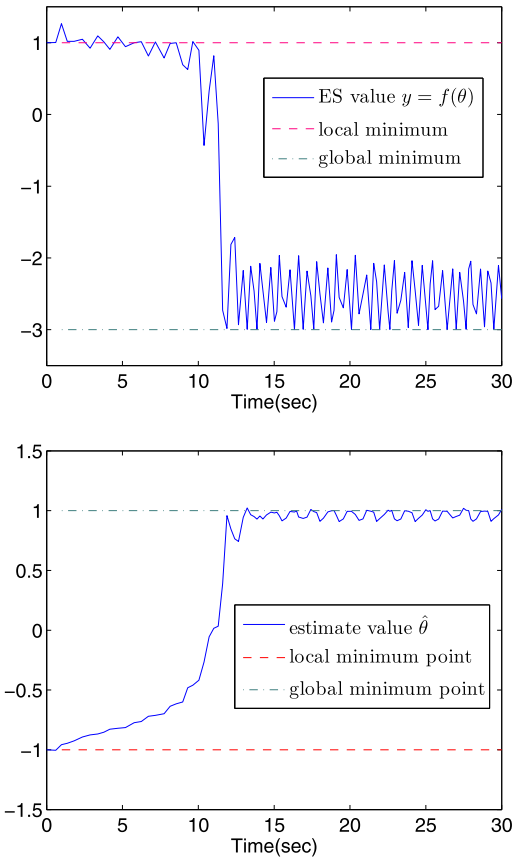

Fig. 2.3 Time response of a discrete-time version of the deterministic extremum seeking algorithm in Fig. 2.2, starting from the local minimum, $\hat{\theta}(0) = -1$. The parameters are chosen as $\omega = 5$, $a = 0.4$, $k = 1$

minimum $\theta = 1$. However, if the amplitude a and the gain k were chosen smaller, the algorithm would be unable to overcome the "hump" between $\theta = -1$ and $\theta = 1$ and it would remain stuck at the local minimum.

2.3.2 A Basic Stochastic ES Scheme

Limitations of the deterministic ES scheme include the fact that the perturbation is uniformly bounded (by a), which may highly restrict the algorithm's region of attraction, and the fact that learning using a single-frequency sinusoidal perturbation is rather simple-minded and rare in probing-based learning and optimization approaches encountered in biological systems.

To overcome such limitations of deterministic probing signals, we consider using stochastic probing signals. Sinusoidal signals have two properties that are crucial for extremum seeking: (i) their mean is zero and (ii) when squared, the mean is positive.

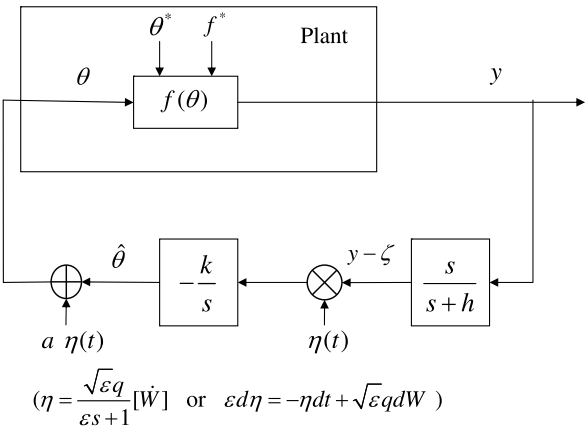

Fig. 2.4 Block diagram for *stochastic* extremum seeking scheme with unbounded perturbations for a static map

Such properties are similar to the properties of Gaussian white noise signals, namely, zero expectation and positive variance.

Hence, we consider replacing the signals $\sin(\omega t)$ in Fig. 2.2 by white noise $\dot{W}(t)$, where $W(t)$ is a standard Brownian motion process (also referred to as the Wiener process). However, such a perturbation is overly aggressive and makes the mathematical analysis intractable because it enters the differential equation in a nonlinear manner (it gives rise to quadratic and other functions of $\dot{W}$).

To soften the impact of the white noise perturbations, while introducing randomness and making the resulting dynamics mathematically tractable, we replace the signals $\sin(\omega t)$ in Fig. 2.2 by the signal $\eta(t)$ obtained by passing white noise $\dot{W}(t)$ through a low-pass filter $\frac{\sqrt{\varepsilon}q}{\varepsilon s+1}$ for some positive constants ε and q, or, given in terms of an Ito differential equation, we employ the perturbation $\eta(t)$ governed by

$$\varepsilon\, d\eta = -\eta\, dt + \sqrt{\varepsilon} q\, dW. \tag{2.2}$$

The resulting stochastic ES scheme is shown in Fig. 2.4.

Figure 2.5 shows the time response of a discrete-time version of the stochastic ES algorithm in Fig. 2.4. Starting from the local minimum $\theta = -1$, the algorithm converges to the global minimum $\theta = 1$.

2.3.3 A Heuristic Analysis of a Simple Stochastic ES Algorithm

To provide the reader with some intuition and motivation, in this section we provide a preliminary and completely informal analysis of the extremum seeking algorithm in Fig. 2.4. We present a series of calculations which, though not reflective of the rigorous methods pursued in the book, do illustrate heuristically the basic ideas behind establishing stability and quantifying the convergence rates of ES schemes.

To simplify our analysis, we eliminate the washout filter from the ES scheme, namely, we replace $\frac{s}{s+h}$ in Fig. 2.4 by a unity gain block. This approximation is

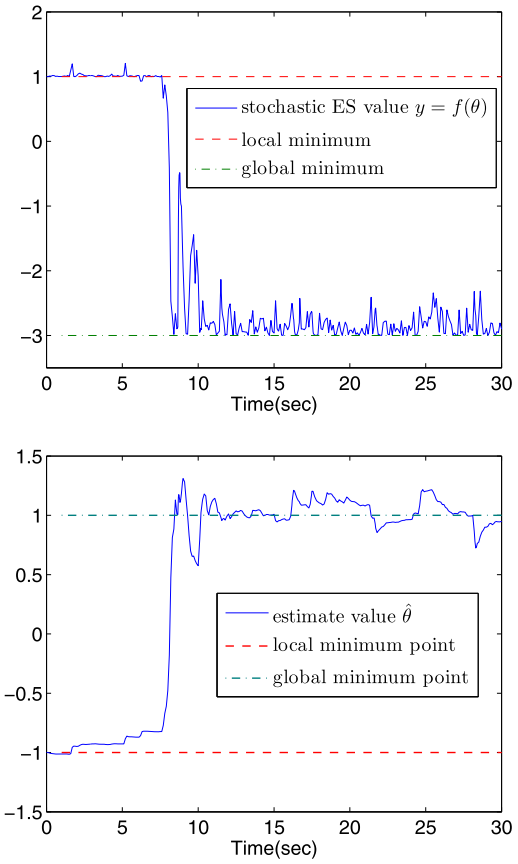

Fig. 2.5 Time response of a discrete-time version of the stochastic extremum seeking algorithm in Fig. 2.4, starting from the local minimum, $\hat{\theta}(0) = -1$. The parameters are chosen as $q = 1$, $\varepsilon = 0.25$, $a = 0.8$, $k = 10$

certainly justified for h that is small relative to other parameters, particularly relative to k. The elimination of the washout filter results in a first-order system, whose sole state is the state $\hat{\theta}$ of the integrator in Fig. 2.4, and which is driven by another first-order linear stochastic system with state η. Despite the low order, the analysis of the closed-loop system is not trivial because the system is nonlinear, time-varying, and stochastic.

We start by introducing notation to describe the system in Fig. 2.4. We note that

$$\theta(t) = \hat{\theta}(t) + a\eta(t) \tag{2.3}$$

and denote the estimation error as

$$\tilde{\theta}(t) = \theta^* - \hat{\theta}(t). \tag{2.4}$$

Combining (2.3) and (2.4), we get

$$\theta(t) = a\eta(t) - \tilde{\theta}(t). \tag{2.5}$$

Then, from the integrator block we observe that the estimation error is governed by

$$\begin{aligned}\dot{\tilde{\theta}}(t) &= -\dot{\hat{\theta}}(t)\\ &= k\eta(t)y(t)\\ &= k\eta(t)f\big(\theta(t)\big).\end{aligned} \tag{2.6}$$

Using (2.5) and applying the Taylor expansion to $f(\theta)$ around θ^* up to second order, we get

$$\begin{aligned}f(\theta) &= f(a\eta-\tilde{\theta})\\ &\approx f\big(\theta^*\big)+f'\big(\theta^*\big)(a\eta-\tilde{\theta})+\frac{1}{2}f''\big(\theta^*\big)(a\eta-\tilde{\theta})^2.\end{aligned} \tag{2.7}$$

Given the assumption that the map $f(\theta)$ has a minimum at θ^*, it follows that $f'(\theta^*)=0$, which yields

$$\begin{aligned}f(\theta) &\approx f\big(\theta^*\big)+\frac{1}{2}f''\big(\theta^*\big)(a\eta-\tilde{\theta})^2\\ &= f\big(\theta^*\big)+\frac{1}{2}f''\big(\theta^*\big)\big[a^2\eta^2-2a\eta\tilde{\theta}+\tilde{\theta}^2\big].\end{aligned} \tag{2.8}$$

Substituting (2.8) into (2.6), we get

$$\begin{aligned}\dot{\tilde{\theta}} &\approx k\eta\left\{f\big(\theta^*\big)+\frac{1}{2}f''\big(\theta^*\big)\big[a^2\eta^2-2a\eta\tilde{\theta}+\tilde{\theta}^2\big]\right\}\\ &= k\eta\left[f\big(\theta^*\big)+\frac{a^2}{2}f''\big(\theta^*\big)\eta^2-af''\big(\theta^*\big)\eta\tilde{\theta}+\frac{1}{2}f''\big(\theta^*\big)\tilde{\theta}^2\right].\end{aligned} \tag{2.9}$$

Grouping the terms in powers of η, we obtain

$$\begin{aligned}\dot{\tilde{\theta}}(t) \approx k\Bigg\{&\eta(t)\left[f\big(\theta^*\big)+\frac{1}{2}f''\big(\theta^*\big)\tilde{\theta}^2(t)\right]\\ &-\eta^2(t)af''\big(\theta^*\big)\tilde{\theta}(t)\\ &+\eta^3(t)\frac{a^2}{2}f''\big(\theta^*\big)\Bigg\}.\end{aligned} \tag{2.10}$$

The signal $\eta(t)$ is a stochastic perturbation governed by the stochastic linear differential equation (2.2), where $W(t)$ is the Wiener process. With small ε, the signal η is a close approximation of white noise. Using elementary Ito calculus, it is easy to calculate the expectations of the three powers of η appearing in (2.10). These expectations have the properties that

$$\lim_{t\to\infty} E\big\{\eta(t)\big\}=0, \tag{2.11}$$

$$\lim_{t\to\infty} E\big\{\eta^2(t)\big\}=\frac{q^2}{2}, \tag{2.12}$$

$$\lim_{t\to\infty} E\big\{\eta^3(t)\big\}=0. \tag{2.13}$$

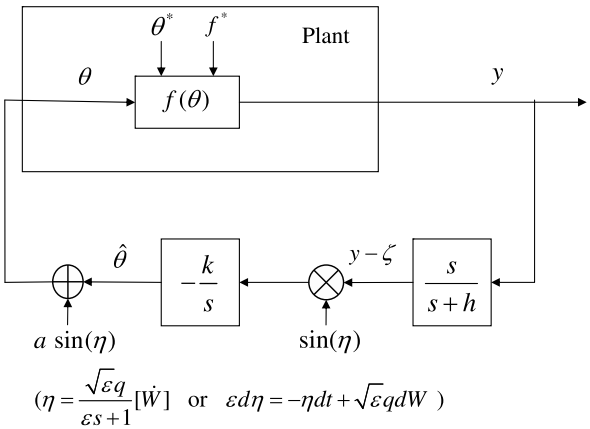

Fig. 2.6 Block diagram for *stochastic* extremum seeking scheme with bounded perturbations for a static map

To illustrate how these relations are obtained, we consider the case of η^2, namely, (2.12), which is obtained by applying Ito's differentiation rule to η^2 with the help of (2.2), which yields the ODE

$$\frac{\varepsilon}{2}\frac{dE\{\eta^2\}}{dt} = -E\{\eta^2\} + \frac{q^2}{2} \tag{2.14}$$

The solution of the linear ODE (2.14) is

$$E\{\eta^2(t)\} = e^{-2t/\varepsilon}E\{\eta^2(0)\} + \frac{q^2}{2}\left(1 - e^{-2t/\varepsilon}\right) \tag{2.15}$$

$$\to \frac{q^2}{2} \quad \text{as } t \to \infty. \tag{2.16}$$

When ε is small, it is clear from (2.15) that the convergence in time t is very fast. This is the case with the convergence rates of all three expectations given in (2.11), (2.12), and (2.13).

Approximating now the η-terms in (2.10) by their respective expectations, after a short transient whose length is $O(\varepsilon)$, the estimation error is governed by

$$\dot{\tilde{\theta}}(t) \approx -\frac{kaq^2}{2}f''(\theta^*)\tilde{\theta}(t). \tag{2.17}$$

This completes our heuristic preliminary study of stability of the stochastic ES scheme in Fig. 2.4. Local stability is expected, in a suitable probabilistic sense, provided $ka > 0$ and provided the map has a minimum at θ^*. Moreover, the convergence speed is governed by the values of the parameters k, a, q, and also by the value of $f''(\theta^*) > 0$. The "flatter" the extremum, the slower the convergence and, conversely, the "sharper" the extremum, the faster the convergence toward it.

Rigorous stability analysis of stochastic ES algorithms is presented in Chaps. 5 and 6. However, the scheme in Fig. 2.4 with the unbounded stochastic perturbation $\eta(t)$ is not amenable to rigorous analysis. To make analysis feasible, using averaging theorems that we develop in Chap. 4, we replace η in the algorithm in Fig. 2.4 by a bounded stochastic perturbation $\sin(\eta)$, obtaining the algorithm in Fig. 2.6.

Algorithms in Figs. 2.4 and 2.6 have very similar local convergence properties. The convergence speeds of the two algorithms are related as

$$\frac{\text{speed}_{\sin(\eta)}}{\text{speed}_{\eta}} = \frac{(1 - e^{-q^2})}{q^2}. \tag{2.18}$$